The Free Form XR Photovoltaic Concentrator: a High Performance SMS3D Design

Aleksandra Cvetković[a], Maikel Hernandez[b], Pablo Benítez[a,b], Juan C. Miñano[a,b], Joel Schwartz[c], Adam Plesniak[c], Russ Jones[d], David Whelan[e]

a CEDINT Universidad Politécnica de Madrid (UPM) ETSI Telecomunicación (IES-205), C. Universitaria, 28040 Madrid, Spain; [b]LPI Europe, Marques de Urquijo 14 5D, 28008 Madrid, Spain; [c] Boeing Satellite Development Center; The Boeing company Phantom Works, 2260 Imperial highway, El Segundo, CA 90245, USA; [d]The Boeing Company , 5301 Bolsa Ave, Huntington Beach, CA 92647, USA; [e]Boeing Integrated Defense Systems, Boeing Phantom Works, 2800 Westminister, Seal Beach, CA, 90740, USA

ABSTRACT

A novel photovoltaic concentrator is presented. The goal is to achieve high concentration design with high efficiency and high acceptance angle that in the same time is compact and convenient for thermal and mechanical management [1].

This photovoltaic system is based on 1 cm^2 multi-junction tandem solar cells and an XR concentrator. The XR concentrator in this system is an SMS 3D design formed by one reflective (X) and one refractive (R) free-form surfaces (i.e., without rotational or linear symmetry) and has been chosen for its excellent aspect ratio and for its ability to perform near the thermodynamic limit. It is a mirror-lens device that has no shadowing elements and has square entry aperture (the whole system aperture area is used for collecting light). This large acceptance angle relaxes the manufacturing tolerances of all the optical and mechanical components of the system included the concentrator itself and is one of the keys to get a cost competitive photovoltaic generator.

For the geometrical concentration of 1000x the simulation results show the acceptance angle of ±1.8 deg. The irradiance distribution on the cell is achieved with ultra-short homogenizing prism, whose size is optimised to keep the maximum values under the ones that the cell can accept.

The application of the XR optics to high-concentration is being developed in a consortium leaded by The Boeing Company, which has been awarded a project by US DOE in the framework of the Solar America Initiative.

Keywords: nonimaging, concentrator, photovoltaic, solar energy, SMS3D

1. INTRODUCTION

The design of photovoltaic concentrators introduces a very specific optical design problem, with features that make it different from any other optical design. It has to be efficient, suitable for mass production, capable for high concentration (for high cell cost not smaller than 1000x), insensitive to manufacturing and mounting inaccuracies, and capable to provide uniform illumination on the cell.

When high concentration is needed (500-1,000x), as occurs in the case of high efficiency multijuction cells, it is likely that it will be crucial for commercial success at the system level to achieve such concentration with a sufficient acceptance angle. This allows tolerance in mass production of all components, relaxes the module assembling and

system installation, and decreasing the costs of the structural elements. Since the main objective of concentration is to make solar energy inexpensive, there can be used only a few surfaces. Decreasing the number of the elements and achieving high acceptance angle, can be relaxed optical and mechanical requirements, such as accuracy of the optical surfaces profiles, the module assembling, the installation, the supporting structure, etc.

This paper presents one of the possible designs that are capable of meeting all the previously mentioned conditions. The free form XR was developed for automotive applications [2], and its adaptation and optimization has been done in the framework of the DOE program Solar America Initiative, in a consortium led by The Boeing Company. The general goal of the program is to develop cost-effective and high efficient system.

As the whole family of the XR, this concentrator also consists of one reflective (X) and one refractive (R) surface. It is very compact design that works near thermodynamical limit of concentration (i.e. it has high concentration and high acceptance angle). In the Figure 1 can be seen the cross section of the proposed design.

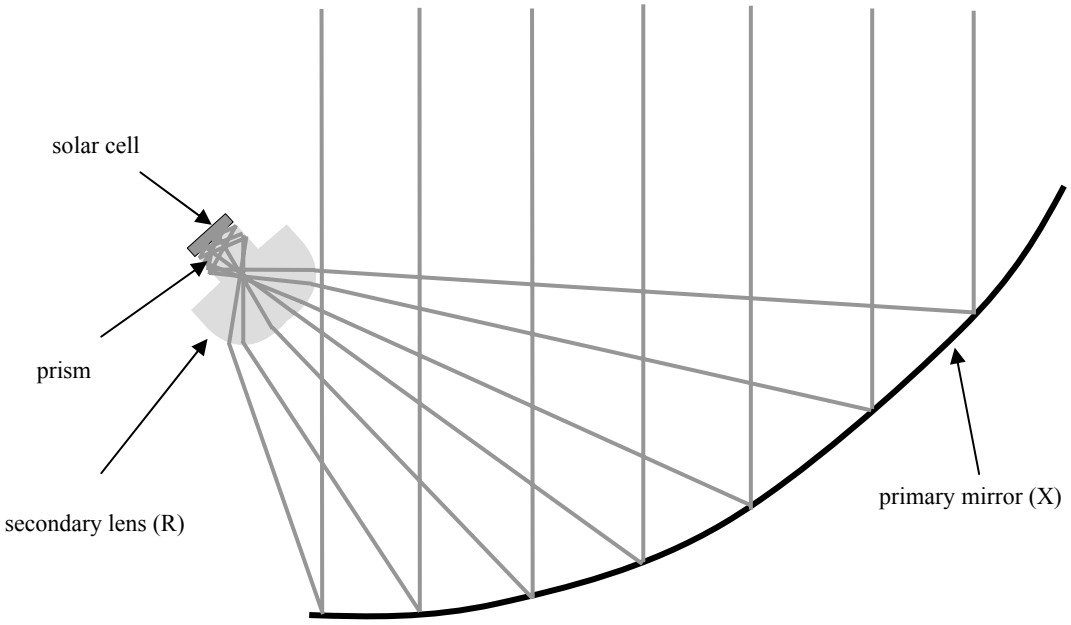

Figure 1 Cross section of an XR SMS3D concentrator

In general, the use of a first reflective surface can reduce notably the aspect ratio of the concentrator at the expense of increasing the optical losses (compared to Fresnel lenses) by the shadowing of the rest of system, as the case is in the conventional rotational XR design (see Chapter 8 in ref [3]). The XR presented here is very asymmetric such that this shadowing is completely avoided. In order to achieve high efficiency and high acceptance angle - concentration product with this asymmetric configuration, conventional XR rotational symmetric optics is not suitable. That is the reason why this XR is designed with the SMS 3D design method [1]. The SMS is the most advanced design method in nonimaging optics [3], which is the branch of optics dealing with maximum efficiency light transfer problems. The design achieves the advantages of an XR, this is, low aspect ratio, good optical efficiency and large acceptance angle. Therefore, the XR concentrator is the first free form photovoltaic device that works near thermodynamic limits of concentration, i.e. achieving an acceptance angle close to the theoretical maximum determined by its concentration. This large acceptance angle relaxes the manufacturing tolerances of all the optical and mechanical components of the system included the concentrator itself and is one of the keys to get a cost competitive photovoltaic generator.

2. FREE-FORM XR CONCENTRATOR

From the name of the device it can be concluded that the rays coming from the sun hit the mirror surface (X) and being reflected towards the lens (R) where they are being refracted towards the receiver. The cell is optically adhered to the end of the short transparent rod, preferably glass, which can be molded in one piece with the free-form lens. The rod may be mirror coated in a secondary operation so that wider-angle rays that enter the rod but would miss the photovoltaic cell are reflected onto the cell. [1]

Alternatively, the rod may reflect by total internal reflection (TIR), alone or in combination with a additional reflector separated from the rod by a narrow air (or low-index dielectric) gap. A rod of suitable length can defocus the reflected rays away from the solar image formed by direct rays. The rod is just long enough to produce a desired degree of defocusing, as it is going to be shown later. As shown in the Figure 2, TIR at point P is possible for any ray beyond the critical angle $\theta_c=\sin^{-1}(1/n)$ (where n is refractive index of the secondary lens), that limits how close to surface normal the interior rays can hit the rod's sides and not escape. For a rod with sides with draft angle γ (as shown in Figure 2) and when the angle of incidence is $\theta=\theta_c$ then the angle β (the angle that incoming rays enter to the rod) is $\beta= 90º-\beta-\gamma$.

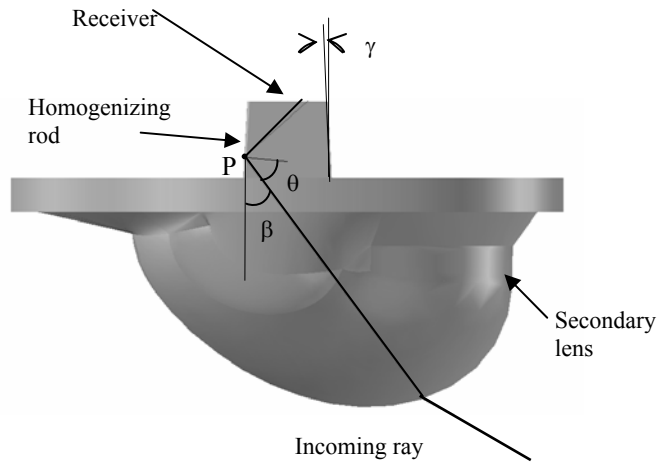

Figure 2 Secondary lens with mixing rod

This prism is a well known homogenizing device in Nonimaging optics and is based on the same principle as the kaleidoscope. Homogenizing rods are commonly used in CPV system [4][5][6][7][8][9] but their length is usually much longer than the cell size (typically 4-5 times) while in the XR the rod can be much shorter (from 0.5 to 1 times the cell size). The sufficiently good homogenization in a short length is possible because the illumination angle of the cell in the XR is very wide.

In SMS 3D design method the optical prescription is stated as incoming and outgoing wavefronts. The optical design consists generally of at least two free form surfaces, calculated numerically by the SMS 3D method, that couple the outgoing and incoming wavefronts with each other. The created surfaces can be refractive or reflective. The full optical system may consist of any number of surfaces that exist before, after or in between the SMS 3Dsurfaces. The effect of these extra surfaces is taken into account by propagating the source and target wavefronts through those surfaces and using the resulting wavefronts as input for the SMS 3D calculation. Besides the obvious physical limitations (i.e. etendue conservation [11][10]), the only condition for a successful SMS 3D design process is the absence of any caustics of the wavefronts to be coupled in the vicinity of the space to be occupied by the SMS 3D surfaces.

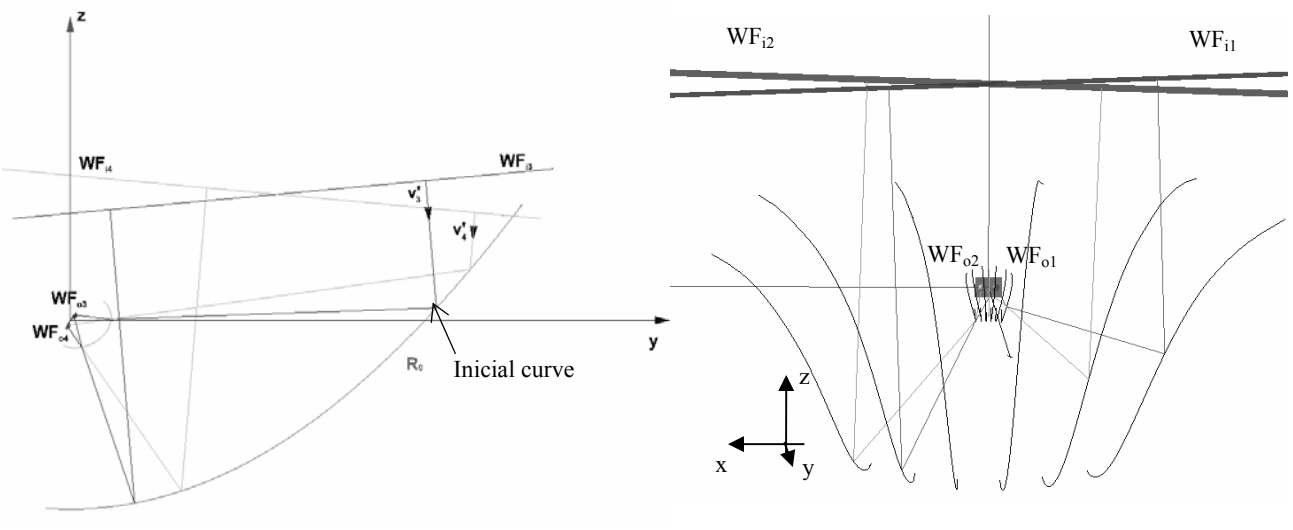

Figure 3: Schematic design procedure for the XR SMS design. Left: 2D design to create seed curve. Right: 3D design that creates SMS "chains" of points in space.

In the XR design the two optical surfaces to be calculated by SMS 3D are a refractive "dome" that is in optical contact with the exit aperture of the homogenizing rod and a reflective mirror surfaces. The two surfaces will couple two source wavefront WF_{i1} and WF_{i2} with two exit wavefront WF_{o1} and WF_{o2} (see Figure 3). Before the 3D SMS calculation can be carried out, a "seed" curve in space can be chosen as a free input parameter. One of the 3D SMS surfaces will start to "grow" from this curve. In the definition of the seed curve lays an important degree of freedom: it can be obtained by a separate simpler 2D SMS calculation using for example WF_{i1}/WF_{o1} and a third pair of wavefronts WF_{i3}/WF_{o3} or if it is necessary even the fourth pair of wavefront that makes easier to control the seed curve construction, WF_{i4}/WF_{o4} (Figure 3). The outgoing wavefronts should describe, how the cell, or in this case the homogenizing rod entry aperture, is going to be illuminated. Although the 3D SMS design does not make use of the third (nor the fourth) wavefront pair but for the seed curve generation, it maintains the coupling of the third wave front pair in surface regions at least in the vicinity of the seed curve, in most practical cases over the entire design. The 3D SMS calculation has two pairs of wavefronts as input parameters, defined as 3D surfaces and two optical path lengths between the two corresponding pairs of wavefronts. In the shown XR design, two outgoing wavefronts are spherical surfaces (WF_{o1} and $WF_{o2)}$ emitted from the two "horizontal" corners of the rectangular entry aperture of the homogenizing prism. The two corresponding incoming wavefronts WF_{i1} and WF_{i2} are chosen to describe the sun illumination. In the shown example those wavefront are planar, rotated by a small angle to the left and right from the optical axis respectively; that angle describes the acceptance angle of the concentrator.

The calculations are carried out by proprietary software. SMS points generated using the four design wavefronts from a point on the seed curve are called chains. The seed curve can be sampled at as many points as desired to create many chains. The full design is eventually defined by all the SMS points that can be interpolated by two 3D surfaces; one of them contains the seed curve.

In Figure 4 can be seen obtained SMS 3D design of XR concentrator.

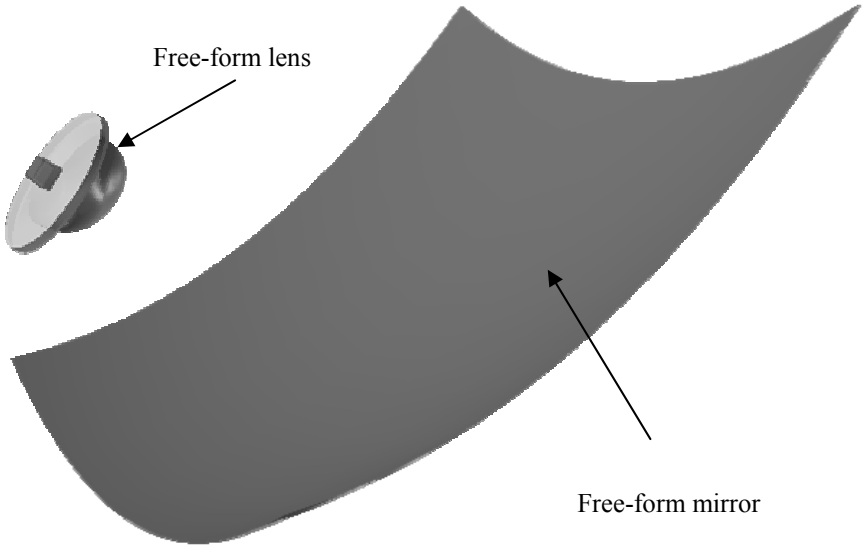

Figure 4 Isometric view of designed XR concentrator

3. RAYTRACE RESULTS

Analyses of described concentrator have been done by raytracing with the objective to determine the angular transmission, optical efficiency and irradiance distribution on the concentrator exit aperture. Additionally, the tolerances of the system have been analysed, i.e. the effect of the misalignment of the system on the optical efficiency, acceptance angle and irradiance distribution on the cell.

3.1 Transmission curves and irradiance distribution on the solar cell

One of the characteristics needed for the evaluation of the concentrator optical performance is the angular transmission of the concentrator. The angular transmission is defined for a given incident beam of parallel rays as the power reaching the cell surface over the power incident on the concentrator aperture (i.e. the optical efficiency as function of the angle of incidence of the parallel beam). For this calculation we assume all the rays in the parallel beam with the same radiance. The solar direct radiation can be modeled as a set of parallel beams (with the same radiance) whose directions point inside the solar disk. The angular radius of the solar disk is 0.26 deg.

Two important merit parameters of the concentrator are derived from the angular transmission curve: the optical efficiency (η_{opt}) and the acceptance angle (α).

The optical efficiency of the concentrator is the maximum value of the angular transmission which uses to happen when the angle of incidence is equal to zero (normal incidence). Notice that the power reaching the cell is not necessarily the power entering into the cell because the cell coating may reflect part of the radiation. There is not a single definition for the optical efficiency. The definition that we use here is power on the cell surface (not inside the cell) over the power of a parallel beam reaching the entry aperture.

The acceptance angle is the angle between the direction at which the angular transmission peaks and the direction at which the optical efficiency falls down to a 90% of the maximum.

The transmission function T gives for any incident beam of parallel rays the percent of power that reaches the cell surface, assuming that any ray of a parallel beam has the same radiance. The direction of the incident parallel beam can

be determined with 2 direction cosines (p,q). Thus, in general T is a function T(p,q). The transmission curve in the x-section is the function T(0,q) and the transmission curve in the y-section is T(p,0). Figure 5 explains both sections.

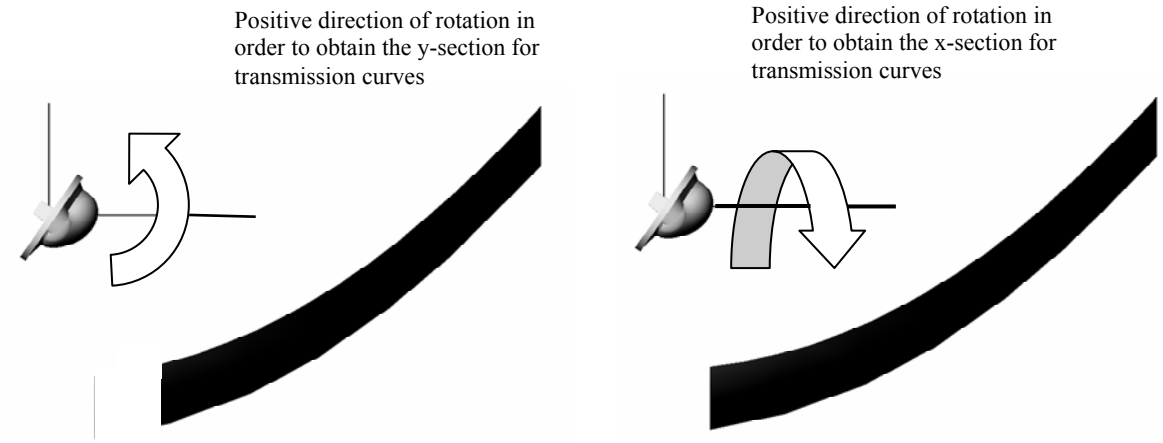

Figure 5 Definition of cross sections for transmission curves

In practice, instead of representing T(0,q) or T(p,0) we represent T(α) where a is either arcos(p) or arcos(q), depending on the type of section.

The Figure 6 gives the transmission curves for both sections.

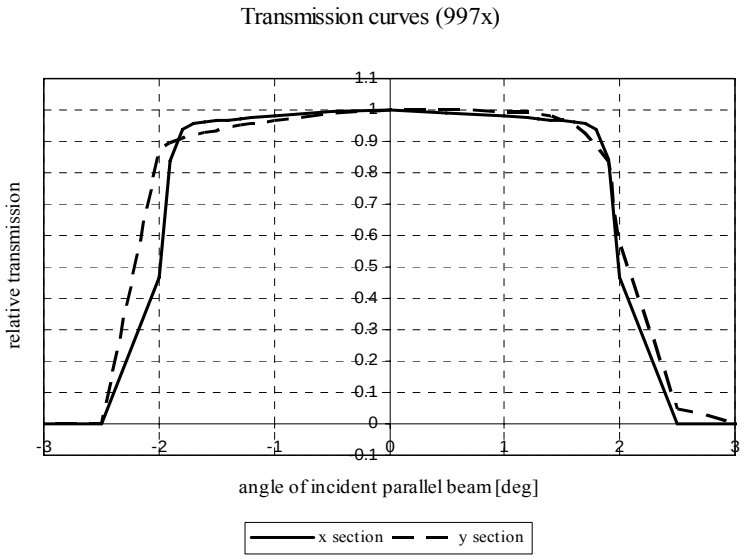

Figure 6 Transmission curves at nominal position

Sometimes the relative angular transmission is calculated taking into account the angular size of the sun instead of using a beam of parallel rays. This is a straight forward way to show the concentrator angular performance under more realistic conditions. In this case the resulting relative angular transmission is a convolution of the sun size with the relative angular transmission calculated using a parallels ray beam. This is the case for the analyses of the irradiance distribution on the solar cell. For the centered sun and assumed input irradiance of 900 W/m^2 the peak irradiance was 907x.

The behavior of XR SMS 3D concentrator can be resumed by:

- Concentration ratio C_g=997.97x ($C_g=A_{entry\ aperture}/A_{exit\ aperture}$; exit aperture area=mixing rod aperture area)

- Optical efficiency η_{opt} (includes Fresnel losses, transmission of the cover and mirror reflectivity): 82.12%;
- Acceptance angle (the nominal transmission curves are shown in Figure 6)
  - ✓ x section ±1.84 deg
  - ✓ y section ±1.81 deg
- Peak irradiance on the cell 907x. (Figure 7)

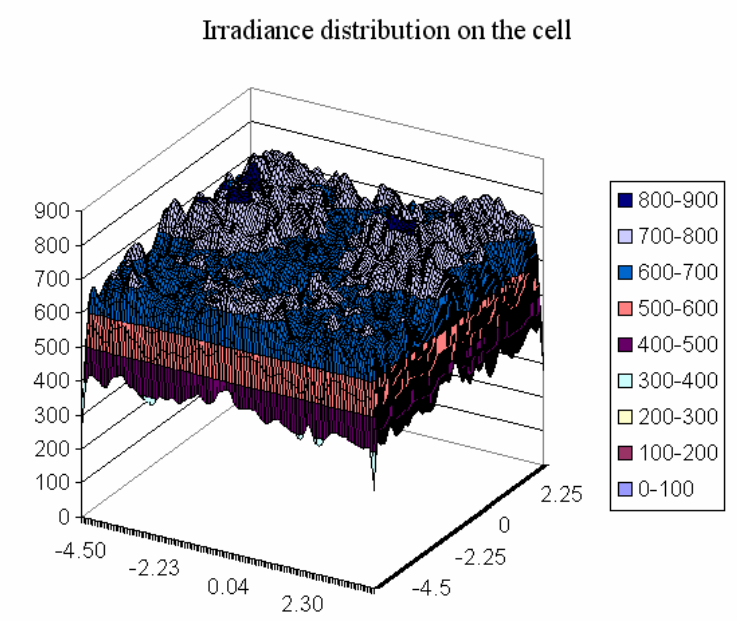

Figure 7 Irradiance distribution on the cell (suns)

For the geometrical concentration (ratio of exit and entry aperture area) of 997x the simulation results show the acceptance of ±1.81 deg to be compared, for instance with a classical photovoltaic concentrator using a Fresnel lens with the secondary system typically has ±0.7 deg of acceptance for 300x of geometrical concentration (see for example the Guascor Foton, Amonix type system [12] with geometrical concentration of 316x and acceptance angle ±0.7º or Concentrix that for geometrical concentration of 385x has the ±0.5º of acceptance angle [13]).

4. CHARACTERIZATION OF XR

The technologies that are used for the mass production are well known in the automotive industry. The primary mirror is manufactured by injection molding, which is a low cost technology that is being used in the automotive industry for headlamps and rear lamps. Some aspects of fabrication have synergies with the DVD and CD industry too. The secondary lens, which is also used for the encapsulation of the cell, is fabricated by glass molding technique.

For free-form optical surfaces, the design, and mold tooling are more complex. However, the cost of mass produced parts is not necessarily higher (since the mold amortization is a small fraction of the part cost).

Tolerances for the primary mirror are significantly relaxed compared to a conventional CPV mirrors, due to the high acceptance angle of the concentrator. The accuracy required for the secondary lens is even smaller than that of the primary, due to the combination of the fact that is a refractive element and that this lens works with high local acceptance angle values (see Chap.14 in ref. [3]).

4.1 Profile measurements

The first prototype has been produced, and have been proceeded the profile measurements of the parts. For the primary mirror the mean distance of measured points from designed surface is 152 microns. Point deviation from the surface is shown in Figure 8. The profile measurements of the secondary lens show that difference between measured points and theoretical surface is less than 150 microns (Figure 9).

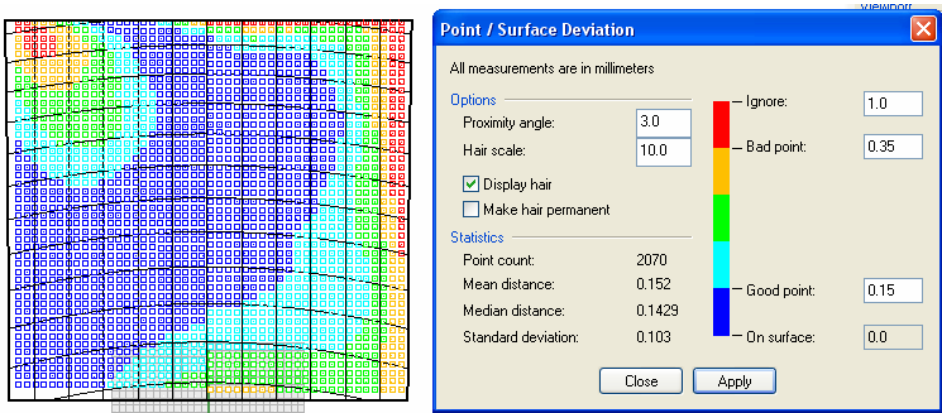

Figure 8 POE profile measurements

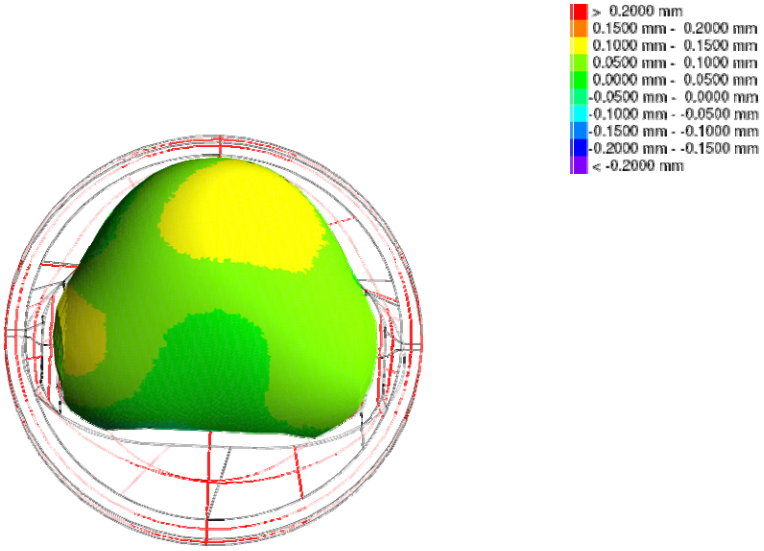

Figure 9 SOE profile measurements

The convex curvature radii in the intersection of the homogenizing rod walls were measured, see Figure 10. This measure was done in a constant plane. The draft angle of the prism walls was also measured; the resulting angle is around 2deg.

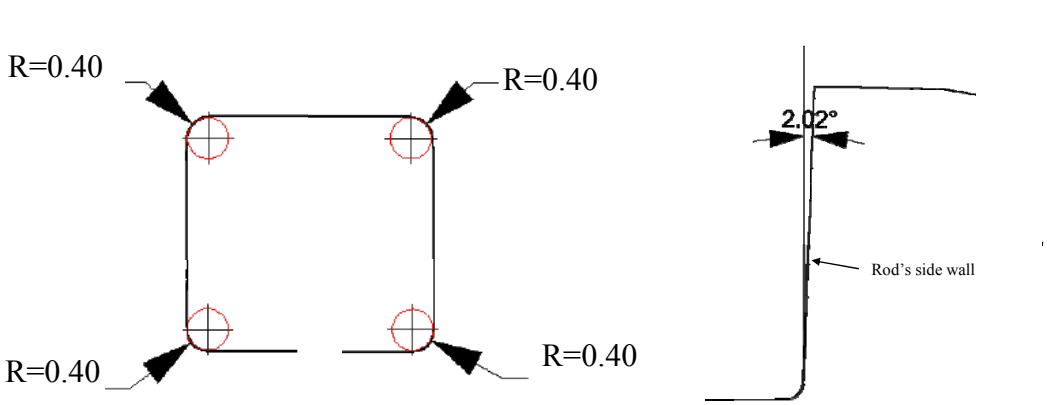

Figure 10 Measurement results of the homogenizing rod's convex curvature radii; left: homogenizing rod's exit surface; left: vertical section of the rod

In order to model the effect of mentioned deviations on the behaviour of the system, has been done the raytrace analysis of the measured profile. The results don't show any change of the efficiency of the system, but is detected the drop of acceptance angle to 1.72 degrees (Figure 11).

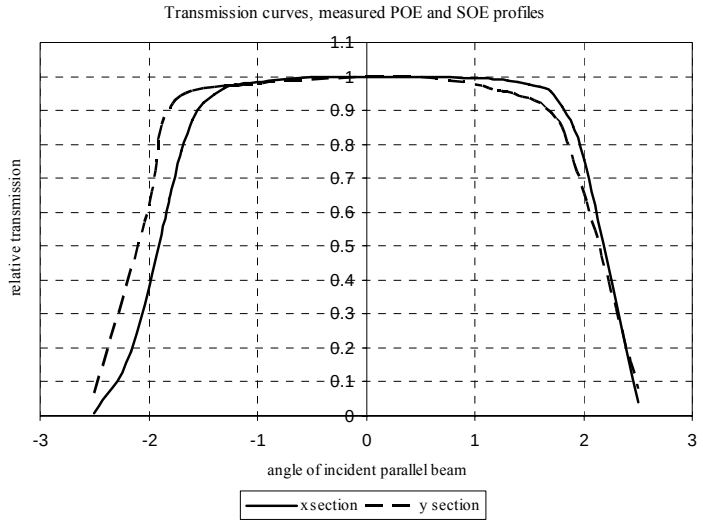

Figure 11 Simulated transmission curves of measured profiles of primary mirror and secondary lens

4.2 Optical measurements

For the characterization of the system and its components was necessary to measure reflectivity of the mirror, Fressnel reflection and absorption of the secondary and transmission of the cover. The measurements have been done with He-Ne laser (635nm) in order to check the behaviour of the materials for this wavelength. As a receiver has been used a photodiode. Measuring points are shown in the schematic presentation in Figure 12 (PD_1 to PD_5).

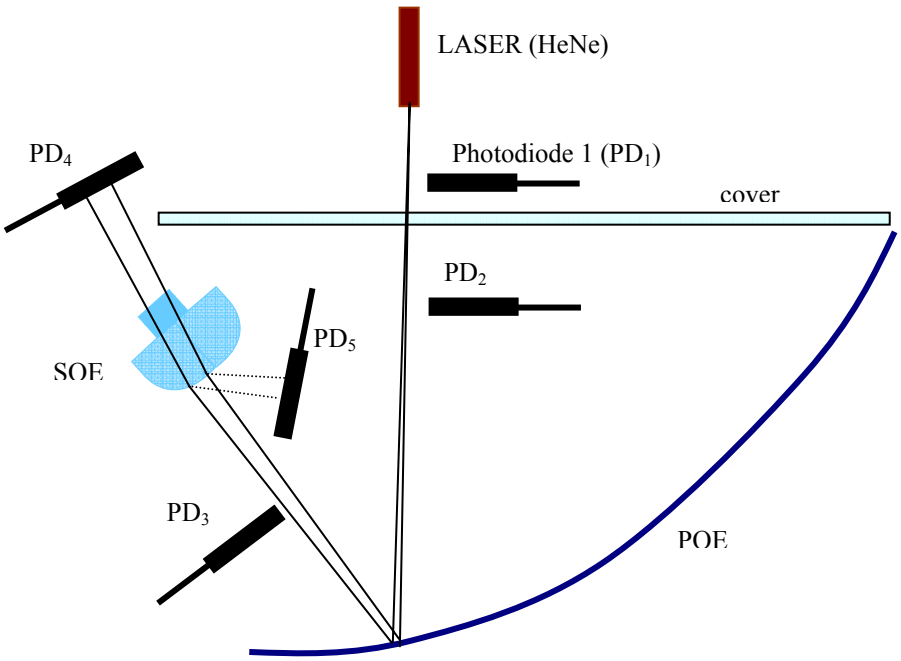

Figure 12 Schematic presentation of measurement equipment

The reflectivity of the mirror was calculated as PD_3/PD_2, the cover transmission as PD_2/PD_1, the Fressnel reflection as PD_5/PD_3 and absorption of the secondary lens as PD_4/PD_3. Finally the optical efficiency of the system is PD_4/PD_1. In order to check the possible dispersion on the surfaces, also have been proceeded the measurements of each component impinging directly the laser beam into them and measuring the reflected or transmitted value. In the Table 1 are shown the results of measurements, and can be seen that the real system behaves close to the designed one.

Table 1 Optical measurements results

Cover transmission	Without anti-reflective coating	With anti-reflective coating
	89.5%	98.11%
Mirror reflection	95.20%	
Secondary lens transmission	94.70%	
	Fressnel reflection	3.01%
	Secondary lens absorption	2.29%
Efficiency of the system	Without anti-reflective coating	With anti-reflective coating
	80.68%	88.45%

In Figure 13 can be seen the graphical presentation of losses distribution through the system. Values shown are relative ones. It can be seen on the left that if we assume 100% of the radiation gets to cover, 91% arrives to the mirror of which are being lost 4.55% due to the reflectivity of the mirror, so that only 86.5% get to the lens. The simulated losses for glass show that the absorption and Fressnel reflection losses are 5.46% of the available light, what means that on the cell we have 81.04%. On the right of the same figure, can be seen measured values in the system. Comparing the values on the left and on the right can be seen that the losses in the real system are 0.36% bigger than expected.

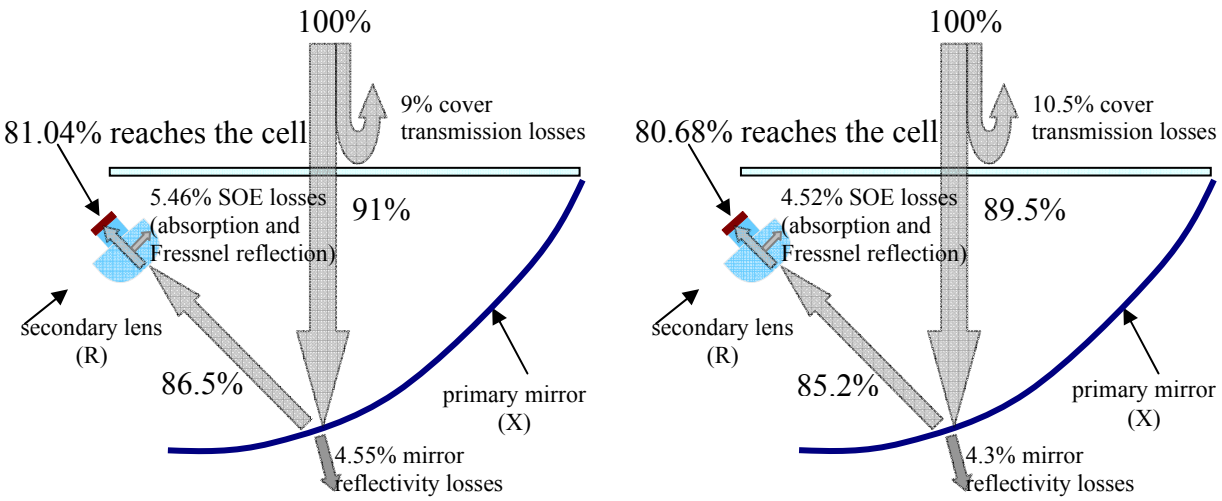

Figure 13 Graphical presentation of the losses distribution in the system: designed (left) and measured (right) values for the parts.

5. CONCLUSIONS

The novel free-form XR concentrator for high efficiency multi-junction solar cells has been presented. It has been designed using the simultaneous multiple surface design method in three dimensions, which is one of the most advanced techniques in nonimaging optics. The designed XR is a compact device that works near thermodinamical limit of concentration, i.e. it has a high concentration-acceptance angle product. With concentration of 997x is achieved acceptance angle of 1.81º, what relaxes all optical and mechanical requirements, and makes it competitive on the market, by decreasing the production cost. The first prototype was produced and has been characterized.

ACKNOWLEDGMENTS

The authors thank to Spanish Ministry of Industry, Tourism and Trade for the project FIT-330100-2007-49. A.C. would like to thank Spanish Ministry of Science and Innovations (FPU grants program) for their financial support.

REFERENCES

[1] Devices shown in this paper are protected by the following US Patents and US and International Patents pending. 6,639,733; 2001069300; CA2402687; 2003282552; 6,896,381; 20040246606; 20050086032; 2005012951;PCT60703667; "Solar Concentrator for Photovoltaics"

[2] A. Cvetkovic, O. Dross, J. Chaves, P. Benitez, J.C. Miñano, and R. Mohedano, " Etendue-preserving mixing and projection optics for high-luminance LEDs, applied to automotive headlamps," Opt. Express 14, 13014-13020 (2006)

[3] R. Winston, J.C. Miñano, P. Benítez, “Nonimaging Optics”, (Elsevier-Academic Press, New York, 2005

[4] H. Ries, J.M. Gordon, M. Laxen, “High-flux photovoltaic solar concentrators with Kaleidoscope based optical designs”, Solar Energy, Vol. 60, No.1,pp.11-16, (1997)

[5] J.J. O’Ghallagher, R. Winston, “Nonimaigng solar concentrator with near-uniform irradiance for photovoltaic arrays” in Nonimaging Optics: Maximum Efficiency Light Transfer VI, Roland Winston, Ed., Proc. SPIE 4446, pp. 60-64, (2001)

[6] D.G. Jenkings, “High-uniformity solar concentrators for photovoltaic systems” in Nonimaging Optics: Maximum Efficiency Light Transfer VI, Roland Winston, Ed., Proc. SPIE 4446, pp.52-59, (2001)

[7] http://www.daido.co.jp/english/rd/7503.pdf
[8] Gen 1 of http://www.solfocus.com/
[9] www.sol3g.com
[10] W. Cassarly, "Nonimaging Optics: Concentration and Illumination", in the Handbook of Optics, 2nd ed., (McGraw-Hill, New York, 2001)
[11] Jung M. Born, E. Wolf, Principles of Optics, (Pergamon, Oxford, 1975)
[12] M.Castro, J. Creixell, *Guascor Foton:Contributions to the manufacturing of concentratior PV system*, 4th International Conference on Solar Concentrators for the Generation of Electricity or Hydrogen, *2007*, El Escorial**,** Spain
[13] H.Lerchenmüller, A.Hakenjos, I.Heile, B.Burger, O.Stalter, From *From FLATCON® Pilot Systems to the first Power Plant*, 4th International Conference on Solar Concentrators for the Generation of Electricity or Hydrogen, *2007*, El Escorial**,** Spain